Physical Properties of Alginate−Starch Cellular Sponges

D. K. Rassis, I. S. Saguy, and A. Nussinovitch*

Institute of Biochemistry, Food Science and Nutrition, Faculty of Agricultural, Food and Environmental Quality Sciences, The Hebrew University of Jerusalem, Israel

The structural and mechanical properties of alginate−starch gel after immersion in sucrose solution was determined. The concentration of the sucrose in the center of the specimen increased exponentially with time. This immersion generally resulted in decreased volume and weight of the wet gels, followed by an increase in relative density of the dried samples and a decrease in their porosity. The population of open and closed pores within the structure of the dried gels was determined, revealing the presence of closed pores, especially at the intermediate time after the beginning of diffusion and before its termination. Compression of the dry gels showed dependency of the strength and brittleness on sucrose diffusion time.

Keywords: *Diffusion; cellular solid; porosity; shrinkage*

INTRODUCTION

Hydrocolloid-based cellular solids can be produced by freeze-dehydration of gels either immediately after their production (Nussinovitch et al., 1993) or after their immersion in different carbohydrate solutions to change their physical and chemical properties (Rassis et al., 1997). The resultant dried cellular solids are an interconnected network of solid struts or plates that form the edges and faces of the sponge cells. Many foods have a cellular solid structure, i.e.: bread, meringue, foamed chocolate, brittle candies, breakfast cereals, and snack food (Gibson and Ashby, 1988). When freeze-drying is used to produce sponges from gels, the water loss from the gel contributes to the creation of pores in the resultant cellular solid. Varying the preparation procedures can modify the mechanical properties of these sponges. For example, internal gas bubbles contained in wet agar gels drastically reduced the mechanical integrity of the dried sponges and affected their porosity. However, the same process in alginate sponges caused only minor mechanical changes (Nussinovitch et al., 1993). Oil included in alginate gels weakened the mechanical strength of the dried sponge, lowered its stress and stiffness at failure as reflected by the deformability modulus, and changed the size distribution and structure of pores of the dried sponge (Nussinovitch and Gershon, 1997). Water plasticization of sponges changes their stress−strain behavior. Vacuum-dried gels or those conditioned to $a_w = 0.33$ collapsed by brittle fracture. Sponges conditioned to $a_w = 0.57$ and 0.75 appeared to collapse by elastic buckling (Attenburrow et al., 1989). In another experiment with four different kinds of bread, the shoulder of the stress−strain curve disappeared in the second and third compression cycles, probably because the closed pores of the bread samples ruptured in the first compression and the cell walls collapsed or fractured (Peleg et al., 1989).

Alginate starch sponges were chosen for this study as the experimental model for tailor-made cellular solids. The opportunity, at least theoretically, to be able to modify the porosity and structure of the dried gels by physical and chemical procedures could furnish a valuable tool for the simulation of a variety of other cellular foods differing in their properties. The porosity of starch products depends on moisture content and the processes utilized. Porosities of 0.06 and 0.27 have been calculated for regular and puffed pasta, respectively (Xiong et al., 1991). White bread and butter cookies have porosities of 0.90 and 0.55, respectively (Hicsasmaz and Clayton, 1992). Porosity and pore-size distribution have a major influence on effective diffusivity (Hicsasmaz and Clayton, 1992; Karathanos and Saravacos, 1993). Thus, such foods could be the focus of this research, especially because other ingredients, such as sweeteners, other fillers, acidity agents, colorants, and minerals can be easily incorporated in the compositions of the gel and be present in its dry structure.

Several recent papers have described different biological, e.g., slow fermentation, and chemical procedures for the production of hydrocolloid sponges (Nussinovitch and Gershon, 1997; Nussinovitch, 1997; Nussinovitch et al., 1998; Reifen et al., 1998). however, less is known about procedures for controlling the physical properties of hydrocolloid sponges to achieve predetermined structural behavior. The main objectives of this study were to demonstrate feasibility (at least in principle); to govern alginate−starch sponge physical properties (e.g., strength, brittleness, and porosity); to study changes in the dry sponges after sucrose diffusion into the wet gel before drying; to study changes in gel dimensions during diffusion; and to evaluate sugar concentration changes with immersion time. This knowledge could ultimately lead to the construction of crunchy products according to specific requirements.

* Corresponding author: Institute of Biochemistry, Food Science and Nutrition, Faculty of Agricultural, Food and Environmental Quality Sciences, The Hebrew University of Jerusalem, P.O. Box 12, Rehovot 76100, Israel (fax 972-8-9476189; e-mail Nussi@agri.huji.ac.il).

S0021-8561(97)01071-6 CCC: $15.00
Published on Web 07/24/1998

MATERIALS AND METHODS

Preparation of Cellular Solids. Cellular solid materials were prepared by dry mix of 15% (w/w) cornstarch (Galam, Kibbutz Maanit, Israel) and 2.5% (w/w) sodium alginate powders, LV [MW $(7-8) \times 10^5$], 61% manuronic acid, and 39% guluronic acid (Sigma, St. Louis, MO) mixed with double-distilled water for 7 h at ambient temperature (25 ± 2 °C). Then, 1.5% (w/w) sodium hexametaphosphate (SHMP; BDH, Poole Dorset, U.K.) was added, and the mixture was further stirred for 30 min and heated to ca. 40 °C, prior to the addition of 1.5% (w/w) $CaHPO_4$ (Riedel-de Haen, Seelze, Germany) that was incorporated for 60 min. The mixture was cooled to 20 ± 1 °C and 3.0% (w/w) fresh glucono-δ-lactone solution (GDL, Sigma) was mixed in. The volume of the GDL solution was approximately 10% of the overall gum solution. The mixture was poured into glass cylinders (2 × 2 cm, diameter × height) and left overnight (15 h) at 4 °C for gelation. The gel samples were immersed in 60 °Bx sucrose solution at ambient temperature (22 ± 2 °C). The volume of the sugar solution was approximately 70 times that of the gel. Immersion periods ranged from 0 to 96 h; samples were removed from the sugar solution, wiped gently, weighed and measured (height and diameter), and stored at −18 °C. The samples were freeze-dried using a pilot plant unit (Model 15 RSRC-X, Repp Industries Inc., Gardiner, NY) operating at 33.3 Pa and −45 °C.

Particle and Bulk Density Determination. The particle density of the cellular solid was determined with a multipycnometer (Quanta Chrome Corp., Syosset, NY). Helium gas was used at a working pressure of 103.4−110.4 kPa. The bulk density was determined by volumetric displacement with glass beads (425−600 μm, Sigma), and porosity was calculated (Marousis and Saravacos, 1990):

$$\epsilon = 1 - (\rho_b/\rho_p) = 1 - \rho_r \quad (1)$$

where ϵ = porosity; ρ_b = bulk density; ρ_p = particle density; and ρ_r is defined as the relative density derived from the ratio ρ_b/ρ_p (Gibson and Ashby, 1988).

After determination of particle and bulk density, the whole sample was pulverized for 4 × 10 s in a coffee mill (Moulinex, Super Junior "S" 505, Reykjavik, Iceland). The new particle density of the powder was redetermined with the multipycnometer and used for deriving the new porosity (total porosity). The difference between the two values was applied to calculate the sample's closed-pores porosity (Lozano and Ubricain, 1980).

Electron Microscopy Micrographs and Image Analysis. Dry gels after sucrose diffusion were the subject of the scanning electron microscopy (SEM) study. These specimens were taken from the same batches from which samples for porosity and mechanical determinations were collected. All specimens fractured due to diffusion or drying were discarded. SEM micrographs were obtained by cutting through the dry cellular solid with a double-edged razor blade and exposing the internal surface features. Single downward cuts were used to produce 2−4 mm slice thickness. A 1:1 mixture of colloidal graphite in isopropyl alcohol and Ducco household glue was used as a conductive mounting adhesive and was mounted on 10 × 10 mm aluminum SEM stubs coated with approximately 50 nm Au/Pd (60:40 w/w) in a Polaron E5100 unit equipped with a Peltier cooling stage. Samples were examined by electron microscopy (Jeol JSM 25S SEM, Tokyo, Japan) at an accelerating voltage of 15 kV and a working distance of 48 mm. Micrographs were magnified at 1000 and 3000. The specific micrographs chosen clearly demonstrated structural changes as a result of physical changes.

Electron micrographs were scanned (Avision scanner, SCSI Model 680) and analyzed on a Macintosh IIsi computer using the public domain NIH image program (written by Wayne Rasband, U.S. National Institutes of Health, Springfield, VA). This program determined the number of pores and their area, measured in pixels and translated into metric units. The smallest measurable area was 0.02×10^{-6} m^2. Three samples from each immersion period (0, 4, and 48 h) were calibrated for pore distribution; the results were calculated and plotted with an Excel (Microsoft Corporation, Soft Art Inc.) software package. The lightest pictures were chosen for scanning and image processing because they were more detailed.

Table 1. Effect of Immersion Time in 60 °Bx Sucrose Solution on Changes in Weight and Volume of Gels[a]

immersion time (h)	weight ratio (W_t/W_0)	volume ratio (V_t/V_0)
1.0	0.86 (± 0.00)	0.83 (± 0.02)
2.5	0.79 (± 0.01)	0.77 (± 0.03)
4.0	0.75 (± 0.01)	0.73 (± 0.01)
6.0	0.70 (± 0.01)	0.67 (± 0.02)
8.0	0.67 (± 0.00)	0.62 (± 0.01)
15.0	0.60 (± 0.00)	0.54 (± 0.01)
23.0	0.57 (± 0.00)	0.51 (± 0.01)
48.0	0.56 (± 0.00)	0.50 (± 0.02)
96.0	0.57 (± 0.00)	0.51 (± 0.01)

[a] Values shown are averages ± standard deviation and were determined in triplicate.

Mechanical Tests. Samples were compressed to 80% deformation between parallel lubricated plates, at a constant deformation (displacement) rate of 10 mm/min, using an Instron universal testing machine (UTM) Model 1011 (Instron Corporation, Canton, MA). The Instron was connected to an IBM-compatible personal computer by an analog to digital conversion interface card. A program developed at the Instron Corporation (Canton, MA) and modified in our laboratory performed the data acquisition and conversion of the continuous voltage of Instron vs time output into digitized stress vs engineering strain relationships:

$$\sigma = F/A_0 \quad (2)$$

$$\epsilon_E = \Delta H/H_0 \quad (3)$$

where σ = stress; ϵ_E = engineering strain; F = the momentary force; ΔH = momentary deformation, $H_0 - H(t)$; and A_0 and H_0 are the cross-sectional area and height of the original specimen, respectively.

The cross-sectional area of a compressed solid sponge specimen rarely expands to any significant extent (Gibson and Ashby, 1988); thus the engineering and "true" stress can be treated as equal for all practical purposes (Swyngedau et al., 1991). Young's modulus was calculated as the slope of the initial linear portion of the stress vs strain curve (Gibson and Ashby, 1988).

Diffusion Measurements. Diffusion of sucrose concentration into the gels was measured by a table refractometer (Carl Zeiss, Berlin, Germany) by removing the samples from the sugar solution and wiping carefully with a paper towel. An inner disk (3 mm height × 8 mm diameter) was taken from the center of the gel, crushed by a mortar and pestle, and diluted with two volumes of distilled water, and total soluble solids (°Bx) were determined. Refractometric values within the gel and the surrounding sucrose solution were also determined vs time of immersion.

Statistical Analyses. Triplicate samples for each treatment were used and the experiments were repeated. Nonlinear regression and one-way ANOVA (Systat version 5.03, Systat Inc., Evanson, IL) were utilized to calculate the effective diffusion and significant differences.

RESULTS AND DISCUSSION

Weight and Volume Changes in Wet Gels. After gelation, the samples were immersed for 0, 1, 2.5, 4, 6, 8, 15, 23, 48, and 96 h in 60 °Bx sucrose solution. Weight loss of the gels during immersion in 60 °Bx sucrose solution, expressed as a weight ratio, W_t/W_0 (weights at immersion time, t, and initial value before immersion, respectively) is listed in Table 1. The average initial weight of the gels was ca. 7.2 g and their

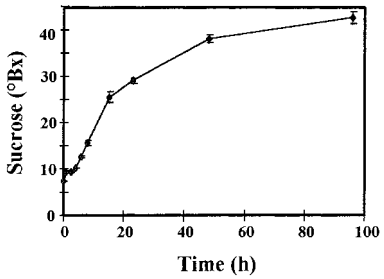

Figure 1. Sucrose diffusion into gels during immersion in 60° Bx sucrose solution.

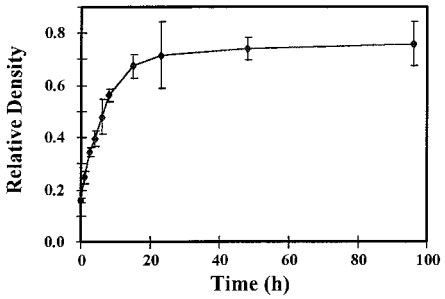

Figure 2. Relative density of dried cellular solid after immersion in 60 °Bx sucrose solution.

volume was ca. 6.2 cm^3. A 14% weight loss was noted after 1 h of immersion. The gel weight ratio decreased to 0.70, 0.60, and 0.57 of the initial values after immersion for 6, 15, and 96 h, respectively. The weight changes in gels were the overall result of water diffusion out of the gel to the surrounding sucrose solution and the penetration of sucrose into the network of the immersed gels. Table 1 also lists the volume ratio V_t/V_0 (volumes at immersion time t and initial value, respectively) and changes in the wet samples' ratio during immersion. The volume ratio decreased to 0.83, 0.67, 0.54, and 0.51 of its original value after immersion for 1, 6, 15, and 96 h, respectively. The volume changes were more prominent (6%) than the weight changes. The changes in volume and weight were caused by a dynamic process as a result of the osmotic pressure differences between the gel and the surrounding medium. This pressure is composed of three forces: rubber elasticity, polymer−polymer affinity, and ion pressure (Tanaka, 1981). The osmotic pressure probably had a higher influence on the volume of samples than on their weight. Volume and weight changes could explain the increase in bulk density and decrease of porosity of the cellular solids after sample freeze-dehydration, as will be demonstrated later.

Sucrose Diffusion during Immersion. After gel specimens were removed from the sucrose solution, the total concentration of soluble solids in the sample core was evaluated. The initial refractometric value of the alginate−starch gels before immersion was 7.5 °Bx due to the total soluble solids within the gel powder, and this value increased due to diffusion to 9.3, 15.6, 25.5, 29.1, 38.1, and 42.6 °Bx after immersion for 1, 8, 15, 23, 48, and 96 h, respectively (Figure 1). The refractometric values after immersion for 48 and 96 h were almost identical, reaching an asymptotic value. Sucrose penetration into the gels was described according to the following diffusion equation for a semiinfinite solid in one direction (Gross and Ruegg, 1987):

$$(C - C_0)/(C_f - C_0) = 2/\pi \sum \{[(-1)^n/(n + {}^1/_2)] \exp[-(n + {}^1/_2)^2 \pi^2 D_{eff} t/L^2] \cos[(n + {}^1/_2)\pi x/L]\} \quad (4)$$

where C, C_0, and C_f are sucrose concentration at a given time t, initial, and final time, respectively; D_{eff} is the effective sucrose diffusivity; and L is the length of the semiinfinite solid in the x direction.

By application of nonlinear regression, the value of the effective diffusivity at the center of the gel was determined. The derived values were $D_{eff} = 4.6 \times 10^{-10}$ m^2/s with an asymptotic standard error of 5.6×10^{-11} and R^2 of 0.997. Similar values, 7.8×10^{-10} and 3.3×10^{-10} m^2/s, were reported for diffusion of glucose (25 °C) into a carrageenan (2%) gel (Hendrickx et al., 1986), and sugar (61%) in an agar gel/milk bilayer system (Warin et al., 1997), respectively.

The calculated overall changes in the gel specimens after immersion for 96 h in 60 °Bx sucrose solution were as follows: sucrose gain, ca. 35% (taking into consideration the initial concentration of soluble solids within the gels); water loss, ca. 77%; and sample shrinkage (as reported above, based on initial volume), 51%.

Osmotic dehydration of fruits is a similar process, where water loss and sucrose gain can be observed. Water loss was shown to be faster than sucrose gain, and the difference grew parallel to increase in concentration of sucrose solution (Erba et al., 1994). Another study on apricot and peach cubes (10 mm) immersed at 45 °C in a 70 °Bx solution for 30 min showed a water loss of 32.1% and 37.7%, fructose gain of 7.7% and 8.8%, and weight reduction of 24.4% and 29.4%, respectively (Shi and Maupons, 1994). Similarly to the gels, fruits during osmotic dehydration suffered from tissue shrinkage and the water and sucrose diffusion were a result of a complex substance migration behavior (Marousis et al., 1989). At the beginning of the immersion, the matrix structure was more porous, and therefore sucrose penetration was easier. As the specimens underwent further shrinkage and more sucrose had deposited and blocked pores (see further discussion), the rate of sucrose penetration was slowed (Rahman and Lamb, 1990). It seems that in our case, a similar process occurred.

Relative Density. The relative density of the samples increased parallel to additional sucrose diffusion into the gels followed by their shrinkage (Figure 2). The relative density of samples not immersed in the sucrose solution was 0.16 (± 0.01). Immersion for 6 h tripled this initial value. The relative density reached a maximum value of 0.76 (± 0.08) after immersion for 96 h. Changes in relative density were faster during the first 15 h of immersion and reached an asymptotic level as immersion time increased. The changes in relative density and sucrose diffusion had the same trend: a fast increase during the first 15 h of immersion, followed by a slower change. The changes in relative density were caused by the diffusion of sucrose into the gels, which explains the exponential behavior of these changes. Applying nonlinear regression analysis yielded D_{eff} of 1.51×10^{-9} m^2/s, an asymptotic standard deviation of 5.6×10^{-11} m^2/s, and $R^2 = 1.00$.

Open and Closed Pores. Diffusion of sucrose into the gels affected the distribution of the open and closed pores in the dried cellular solids. Changes in the porosity of freeze-dehydrated cellular solids after different immersion times are depicted in Figure 3. The figure shows that porosity decreased from an initial

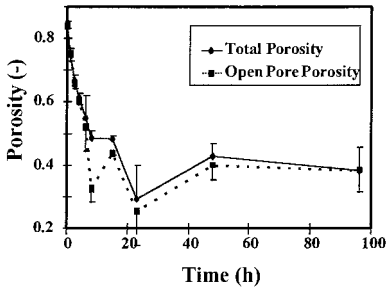

Figure 3. Porosity of open and total pores.

Figure 4. Photograph of dried cellular solids after immersion in 60 °Bx sucrose solution for 0, 4, and 48 h, from left to right. Upper panel shows front view; lower panel shows top view.

value of 0.84 (± 0.01) to 0.38 (± 0.07) after immersion in sucrose solution for 96 h.

The difference between the total porosity and the open-pore porosity is the sum of the closed pores within the structure of the dried specimen. Up to 4 h of immersion, no difference between the total and open porosity was observed. A higher total porosity was observed between 6 and 48 h of immersion. However, only at 8 and 15 h was this difference significant ($P < 0.002$). Between 8 and 15 h of immersion, the specimens' appearance changed from cylindrical to shrunken (Figure 4). The shrinking at mid-sample height and the center of the bases occurred during a few hours, in which a greater number of closed pores was detected. When shrinking was completed and sugar movement (diffusion) continued, the number of closed pores decreased with time.

The particle density of the ground sample should be higher than the particle density of the whole sample if

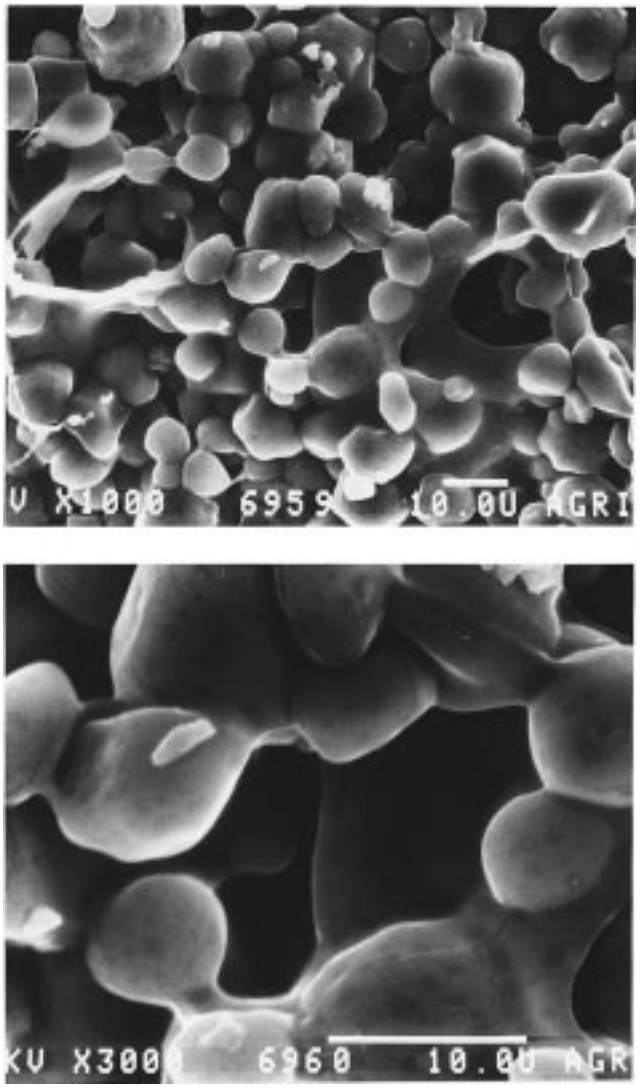

Figure 5. Typical SEM of a cellular solid composed of alginate (2.5%) and starch (15%): upper panel, ×1000 magnification; lower panel, ×3000 magnification. (Figure is reproduced here at 70% of the original.)

there are closed pores with air trapped in them (Lozano and Urbicain, 1980). It should be noted that helium gas, while determining the particle density, may penetrate some of the closed pores, especially in the beginning of the process, when the matrix is not very dense yet (Hinz and Eggers, 1996).

Pore Size Distribution. The pores detected in the dry gels (sponges) were of different size and shapes. The upper panel of Figure 5 (×1000) shows a typical dry alginate−starch gel before immersion in sucrose solution. Many void spaces were detected between the starch (spherelike) granules [$(25-50) \times 10^{-6}$ m] and embedded in the matrix created by the alginate network. A magnified part (×3000) of the same picture (Figure 5, lower panel) shows the void spaces, whereas the starch granules are demonstrated in a clearer manner. Changes in the resultant cellular solid after immersion for 48 h in 60 °Bx sucrose solution are shown in Figure 6, upper panel. Sucrose penetration caused a decrease in void spaces. In addition, a coating "cover" of sucrose wrapping the primary matrix can be seen. The sucrose deposits mostly in an amorphous state (Roos, 1995). This sucrose layer can be better seen in Figure 6, bottom panel, where some folds are distin-

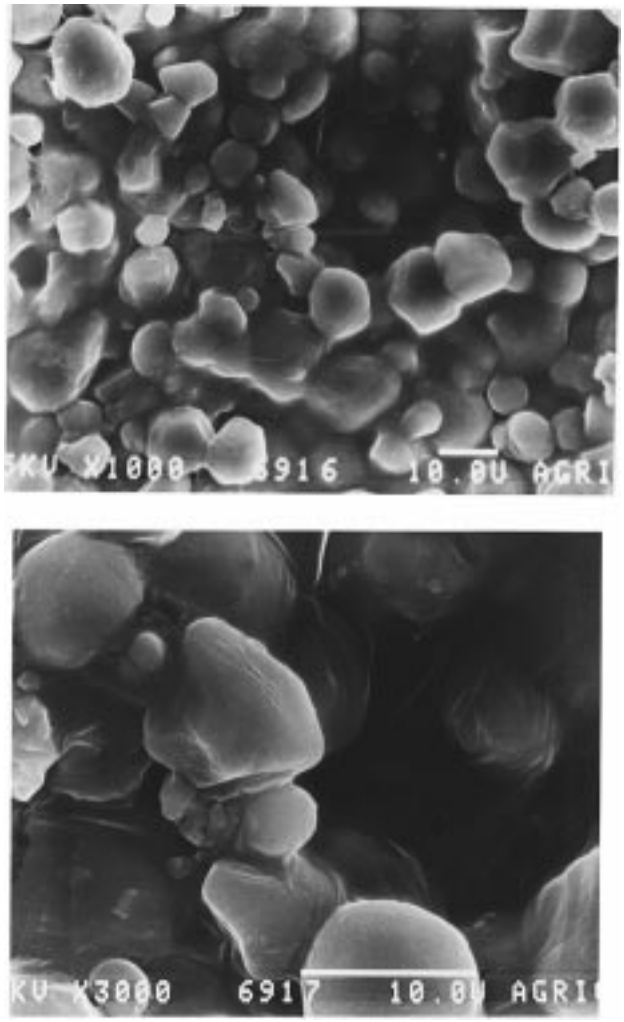

Figure 6. Typical SEM of a cellular solid as above after immersion for 48 h in 60 °Bx sucrose solution: upper panel, ×1000 magnification; lower panel, ×3000 magnification. (Figure is reproduced here at 65% of the original.)

guishable on the surface of the granules. It seems that some of the spherical granules had been changed to more angular shapes by the sucrose deposition, probably as a result of the osmotic pressure. The changes in the cellular solid matrixes, as revealed by volume and weight decrease, are also reflected in the SEM micrographs.

By use of image analysis of the SEM micrographs, the area of the pores was divided into five ranges, and the percentage of each pore area vs the overall area measured was calculated (Figure 7). These analyses were performed with at least three micrographs per treatment. The percentage of the pore area was derived at 0, 4, and 48 h immersion in 60 °Bx sucrose solution. The most porous cellular solid, with the highest percentage of pore area, was detected before immersion (time zero). These sponges had large voids, evidenced by the high percentage of the pore area. Of the two largest pore-area ranges, $(10-100) \times 10^{-6}$ m^2 (entitled D) and $(100-1000) \times 10^{-6}$ m^2 (entitled E), the detected percentages of the voids were 10.19% (± 1.76%) and 24.79% (± 5.93%), respectively. After immersion for 4 h in sucrose solution, the percentage of the void area ranged between 6.59% (± 0.16%) and 15.98% (± 1.67%), respectively. Immersion for 48 h decreased the latter values to 2.17% (± 0.48%) and 12.31% (± 4.56%), respectively. It can also be seen that an increase in

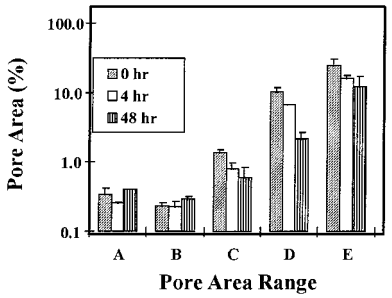

Figure 7. Pore area distribution in cellular solids derived with image analysis: A, $(0.02-0.10) \times 10^{-6}$ m^2; B, $(0.1-1.0) \times 10^{-6}$ m^2; C, $(1.0-10.0) \times 10^{-6}$ m^2; D, $(10-100) \times 10^{-6}$ m^2; E, $(100-1000) \times 10^{-6}$ m^2.

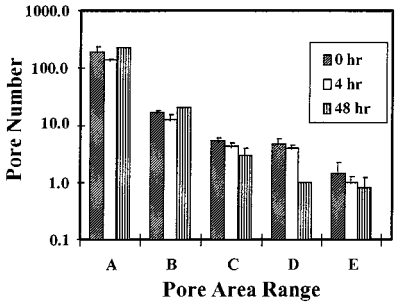

Figure 8. Number of pores in cellular solids of pore area ranges derived with image analysis: A, $(0.02-0.10) \times 10^{-6}$ m^2; B, $(0.1-1.0) \times 10^{-6}$ m^2; C, $(1.0-10.0) \times 10^{-6}$ m^2; D, $(10-100) \times 10^{-6}$ m^2; E, $(100-1000) \times 10^{-6}$ m^2.

immersion time resulted in a significant ($P < 0.05$) change, either decreasing or increasing the percentage of the large pore area and the small pore area, respectively. At the two smallest pore area ranges, namely, $(0.02-0.10) \times 10^{-6}$ m^2 (entitled A) and $(0.10-1.00) \times 10^{-6}$ m^2 (entitled B), pore area percentages were 0.33% (± 0.09%) and 0.23% (± 0.02%), and 0.40% (± 0.00%) and 0.29% (± 0.04%), at time zero or after immersion of 48 h, respectively. A greater number of small pores was detected after immersion for 48 h in sucrose solution than at time zero. As more sucrose molecules diffused into the wet gel matrix, this excess precipitated inside the large pores, so that they became smaller or were apparently filled up. Such an estimation, which can be visualized by the SEM micrographs, explains the high percentage of the large pore area at time zero, followed by a higher percentage of small pore-area after immersion for 48 h.

The number of pores detected at five pore area ranges is depicted in Figure 8. The measurements were performed on micrographs of the dry sponges, and the area examined on each micrograph was 6800×10^{-6} m^2. The pore area was determined for three immersion times (i.e., 0, 4, and 48 h). For all immersion times, the number of pores with the smallest area was much higher than those derived for the larger areas. The largest number of small pores was detected after 48 h of immersion, namely 230.50 (± 0.75) and 20.38 (± 0.38) pores for pore-area ranges defined as A and B, respectively. For the same pore-area ranges, the number of pores were 194.38 (± 48.97) and 16.88 (± 0.88), and 138.22 (± 5.13) and 12.69 (± 2.58), for 0 and 4 h of immersion time, respectively. The number of the large-area pores was small for all immersion times. Increasing immersion time reduced the number of these pores. The number of pores at time zero was 4.75 (± 1.06) and 1.45 (± 0.78) for pore-area range D and E, respectively.

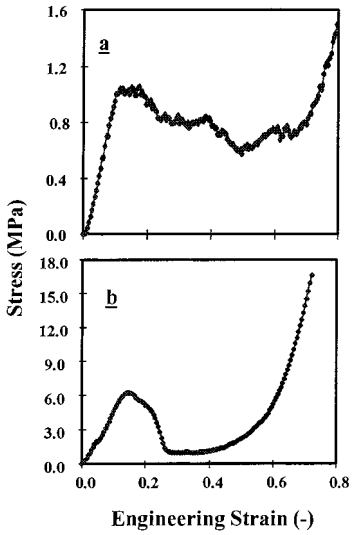

Figure 9. Engineering strain vs compressive stress: (a) no immersion; (b) immersion for 4 h in 60 °Bx sucrose solution.

For these pore-area ranges, the number of pores detected after immersion for 4 and 48 h was 3.92 (± 0.52) and 1.00 (± 0.25), and 1.00 (± 0.00) and 0.78 (± 0.39), respectively. These data indicated that the number of pores occupying a similar area depended on the immersion time of the gel specimens. Immersion time decreased the number of large-area pores and increased the number of small-area pores. However, this effect was not significant ($P < 0.05$) for all cases, probably due to insufficient resolution of the image analysis.

Initially, the sum of all the detected pores was 37% of the analyzed area. Immersion for 4 and 48 h reduced the total pore area to 24% and 16%, respectively. The detected total number of pores at time zero was 223, changing to 160 and 255 after immersion for 4 and 48 h, respectively. Hence, sucrose diffusion into the gel specimens changed the number of detected pores, but the observed overall area of the pores was smaller, likely as a result of the transformation of large pores into several smaller ones.

Sucrose penetration and its deposition in the gel samples resulted in the detection of a greater amount of small pores after freeze-dehydration. This increase was parallel to the increase in immersion time followed by the disappearance of the larger pores. The different approaches, namely, the porosity (determined by bulk and particle density) and the image analysis, yielded different results. In general, the porosity data had higher values than those derived by the image analysis. This disagreement can be explained by assuming that a large number of pores smaller than 0.02×10^{-6} m^2 were not detected by the NIH image-analysis method, while the helium gas was able to penetrate them. Furthermore, the image analysis is limited by its two-dimensional observation capacity.

Stress−Strain Relationship. Dry hydrocolloid cellular samples ("sponges") produced from gels immersed in sucrose solution of 60 °Bx for 0, 4, 48, and 96 h were freeze-dried and compressed by a UTM to approximately 80% deformation. A typical stress−strain relationship of such cellular solids includes three easily observed parts. Similar curves can be obtained for samples not previously immersed in sucrose solution (Figure 9a). The first stage of the curve was linear, indicating that up to a small deformation of ca. 12% the solid behaved as an elastic solid. In the second part of the curve, only relatively small changes in stress (0.6−1.0 MPa) were detected, followed by larger changes in strain (0.1−0.7), possibly a result of cell collapse. The third part of the curve showed a prominent increase in stress with little or no change in strain. The steep increase in stress was a result of densification of the dry matter of which the cellular solid was composed (Gibson and Ashby, 1988).

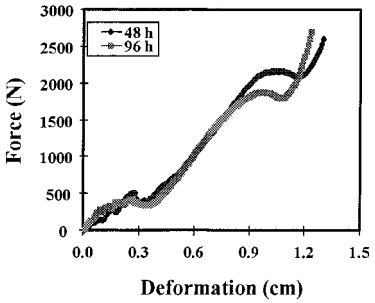

Figure 10. Force vs deformation of cellular solids after immersion in 60 °Bx sucrose solution for 48 and 96 h.

The stress−strain behavior of such cellular solids after the alginate−starch gel was embedded in sucrose solution for 4 h, followed by drying, is presented in Figure 9b. After the diffusion ended, a harder layer of about 2−3 mm that contained sucrose was detected all around the gel. The gel, and later the sponge, comprised an inner core of untouched cellular solid coated by a layer absorbed with sucrose. When this solid was compressed between the lubricated UTM plates, a different sigmoid stress−strain relationship was observed. Up to a level of ca. 0.15 engineering strain, stress increased as expected from such solids due to the sucrose casing. The later reduction in stress may have been caused by the softer texture of the inner solid. It should be emphasized that the cellular solid was much stronger after sucrose diffusion in comparison to the nontreated gel. The maximal stress levels observed for the shoulder in the stress−strain curves were approximately 1.0 and 6.0 MPa for 0 and 4 h of immersion, respectively.

After ca. 15 h, the cylindrical (geometrical) shape of the specimens was lost as a result of uneven contraction of the gel specimens in the sucrose solution (Figure 4); thus, simple analysis of stress−strain relationship was not possible. Consequently, data are presented by force− deformation curves for 48 and 96 h of immersion (Figure 10). For these specimens, the force increased parallel to an increase in deformation. The sucrose content differed only slightly between these two cellular solids; hence their force−deformation behavior was very similar.

Young's Modulus. Young's modulus is defined as the initial slope of the stress−strain curve. Generally, increasing the relative density of the sponge increases Young's modulus, raises the plateau stress, and reduces the strain at which densification begins (Gibson and Ashby, 1988). Before immersion (time zero), Young's modulus was 9.5 ± 3.4 MPa, and it increased 5.1 times after immersion for only 4 h, reaching a value of 48.3 ± 7.9 MPa. Sucrose penetration and sample shrinkage increased the stiffness of the specimens. In general, sucrose diffusion can serve as a tool in monitoring the mechanical and structural characteristics of hydrocolloid cellular solids. Further research on the role of other carbohydrates (e.g., glucose, fructose) is necessary.

In conclusion, the wet gels lost water to their surroundings during immersion in sucrose solution, due to the difference in osmotic pressure, with resultant diffusion of sucrose into the specimen. The overall results of this process were sample shrinkage, weight loss, and decreased porosity. Sucrose diffusion followed an exponential behavior, in which the major changes occurred during the first 15 h of immersion. It is possible that, during sucrose diffusion, closed pores developed. The maximum number of closed pores was detected between 8 and 15 h of immersion. Fluctuation in the number of closed pores was a result of the dynamical nature of the diffusion process. SEM micrographs revealed changes in the matrix during sucrose penetration, followed by transformation of the open structure into a denser and more closed one. Image analysis strengthened these conclusions: a greater amount of large pores was found in the samples not immersed in the sucrose solution. After immersion for 48 h, the number of small pores increased parallel to the decrease in porosity and sample shrinkage. Sucrose penetration into an alginate−starch cellular solid rendered it more brittle and mechanically stronger and stiffer.

LITERATURE CITED

Attenburrow, G. E.; Goodband, R. M.; Taylor, L. J.; Lillford, P. J. Structure, mechanics and texture of a food sponge. *J. Cereal Sci.* **1989**, *9*, 61−70.

Erba, M. L.; Forni, E.; Colonello, A. Influence of sucrose composition and air dehydration levels on the chemical−physical characteristics of osmodehydration fruit. *Food Chem.* **1994**, *50*, 69−73.

Gibson, L. J.; Ashby, M. F. In *Cellular Solids, Structure and Properties*; Pergamon Press: New York, 1988; pp 120−141.

Gross, J. B.; Ruegg, M. Determination of the apparent diffusion coefficient of sodium chloride in model foods and cheese. In *Physical Properties of Foods 2*; Jowitt, R., Escher, F., Kent, M., McKenna, B., Roques, M., Eds.; Elsevier: London, U.K., 1987; pp 71−104.

Hendrickx, M.; Vanden Abeele, C.; Engels, C.; Tobback, P. Diffusion of glucose in carrageenan gels. *J. Food Sci.* **1986**, *51*, 1544−1546.

Hicsasmaz, Z.; Clayton, J. T. Characterization of the pore structure of starch based food materials. *Food Struct.* **1992**, *11*, 115−132.

Hinz, Th.; Eggers, R. Determination of porosity and particle size of natural bulk materials using image analysis. *Nahrung* **1996**, *40*, 116−124.

Hwang, M. P.; Hayakawa, K.-I. Bulk densities of cookies undergoing commercial baking processes. *J. Food Sci.* **1980**, *45*, 1400−1407.

Krathanos, V. T.; Saravacos, G. D. Porosity and pore size distribution of starch materials. *J. Food Engin.* **1993**, *18*, 259−280.

Lozano, J. E.; Urbicain, M. J. Total porosity and open pore porosity in the drying of fruits. *J. Food Sci.* **1980**, *45*, 1403−1407.

Marousis, S. N.; Saravacos, G. D. Density and porosity in drying starch materials. *J. Food Sci.* **1990**, *55*, 1367−1372.

Marousis, S. N.; Karathanos, V. T.; Saravacos, G. D. Effect of sucrose on the water diffusivity in hydrated granular starches. *J. Food Sci.* **1989**, *54*, 1496−1500.

Nussinovitch, A. *Hydrocolloid applications. Gum Technology in the Food and Other Industries*; Chapman and Hall: London, U.K., 1997.

Nussinovitch, A.; Gershon, Z. Alginate−oil sponges. *Food Hydrocolloids* **1997**, *11* (3), 281−286.

Nussinovitch, A.; Velez-Silvestre, R.; Peleg, M. Compressive characteristic of freeze-dried agar and alginate sponges. *Biotechnol. Prog.* **1993**, *9*, 101−104.

Nussinovitch, A.; Gershon, Z.; Peleg, L. Characteristics of enzymatically produced agar-starch sponges. *Food Hydrocolloids* **1998**, *12*, 105−110.

Peleg, M.; Roy, I.; Campanella, O. H.; Normand, M. D. Mathematical characterization of the compressive stress−strain relationship of spongy baked goods. *J. Food Sci.* **1989**, *54*, 947−949.

Rahman, M. S.; Lamb, J. Osmotic dehydration of pineapple. *J. Food Sci. Technol.* **1990**, *27* (3), 150−152.

Rassis, D.; Nussinovitch, A.; Saguy, I. S. Tailor-made porous solid foods. *Int. J. Food Sci. Technol.* **1997**, *32*, 271−278.

Reiffen, R.; Edris, M.; Nussinovitch, A. A novel, vitamin A-fortified, edible hydrocolloid sponge for children. *Food Hydrocolloids* **1998**, *12*, 111−114.

Roos, Y. H. *Phase Transitions in Foods*; Academic Press: New York, 1995; pp 110−119.

Shi, X. Q.; Maupony, P. F. Mass transfer in a vacuum osmotic dehydration of fruits: A mathematical model approach. *Lebens. Wissen. Technol.* **1994**, *27*, 67−72.

Swyngedau, S.; Nussinovitch, A.; Roy, I.; Peleg, M.; Huang, V. Comparison of four models for the compressibility of breads and plastic foams. *J. Food Sci.* **1991**, *56*, 756−759.

Tanaka, T. Gels. *Sci. Am.* **1981**, *244* (1), 110−123.

Warin, F.; Gekas, V.; Voirin, A.; Dejmek, P. Sugar diffusivity in agar gel/milk bilayer systems. *J. Food Sci.* **1997**, *62*, 454−456.

Xiong, X.; Narishiman, G.; Okos, M. R. Effect of composition and pore structure on energy and effective diffusivity of moisture in porous food. *J. Food* **1991**, *15*, 187−208.

Received for review December 16, 1997. Revised manuscript received April 27, 1998. Accepted June 2, 1998.

JF971071T